Interfacial friction damping properties in magnetorheological elastomers

2011 Smart Mater. Struct. 20 035007

(http://iopscience.iop.org/0964-1726/20/3/035007)

Smart Mater. Struct. **20** (2011) 035007 (8pp) doi:10.1088/0964-1726/20/3/035007

Interfacial friction damping properties in magnetorheological elastomers

Yanceng Fan[1], Xinglong Gong[1,3], Shouhu Xuan[1,3], Wei Zhang[1], Jian Zheng[1] and Wanquan Jiang[2]

[1] CAS Key Laboratory of Mechanical Behavior and Design of Materials, Department of Modern Mechanics, University of Science and Technology of China, Hefei 230027, People's Republic of China

[2] Department of Chemistry, University of Science and Technology of China, Hefei 230026, People's Republic of China

E-mail: gongxl@ustc.edu.cn and xuansh@ustc.edu.cn

Received 27 July 2010, in final form 12 November 2010
Published 8 February 2011
Online at stacks.iop.org/SMS/20/035007

Abstract

In this study, the interfacial friction damping properties of magnetorheological elastomers (MREs) were investigated experimentally. Two kinds of carbonyl iron particles, with sizes of 1.1 μm and 9.0 μm, were used to fabricate four MRE samples, whose particle weight fractions were 10%, 30%, 60% and 80%, respectively. Their microstructures were observed using an environmental scanning electron microscope (SEM). The dynamic performances of these samples, including shear storage modulus and loss factor were measured with a modified dynamic mechanical analyzer (DMA). The experimental results indicate that MRE samples fabricated with 1.1 μm carbonyl iron particles have obvious particle agglomeration, which results in the fluctuation of loss factor compared with other MRE samples fabricated with large particle sizes. The analysis implies that the interfacial friction damping mainly comes from the frictional sliding at the interfaces between the free rubber and the particles.

(Some figures in this article are in colour only in the electronic version)

1. Introduction

Magnetorheological (MR) materials belong to a group of smart materials, because their rheological or mechanical properties can be changed continuously, rapidly and reversibly by an applied magnetic field [1–8]. MR elastomers (MREs) are composed of microsized soft magnetic particles and low-permeability elastomer materials. Under an external magnetic field, the particles form an anisotropic ordered pre-configuration such as chains or more complex three-dimensional structures, which are locked into a matrix. MREs are solid-state analogs of MR fluids and a new branch of MR materials. They have both the MR effect and good mechanical performance. Thus, these materials have found promising applications in vibration attenuation and noise control areas. A typical application is to develop adaptive tuned vibration absorbers based on MREs [9–13]. It is noted that the absorber effectiveness of these MRE vibration absorbers depends much on the damping properties (loss factor) of MREs. Low damping leads to high vibration reduction and the better transferring capability of vibration, while high damping results in poor vibration suppression [14, 15]. The study of Sun *et al* [14] indicated that the vibration reduction effect increased obviously when the damping ratio reduced from 0.05 to 0.005. Hoang *et al* [15] also observed this increased tendency of vibration reduction effect as the damping ratio reduced from 0.35 to 0.05. Thus, to further study the absorber effectiveness of MRE adaptive tuned vibration absorbers, it is important to investigate the damping properties of MREs. Unfortunately, very little work has focused on this research. Demchuk *et al* [16] studied the influence of particle size on the loss factor of MREs and found that the loss factor decreased with the increment of particle size. Chen *et al* [17] studied the influences of matrix type, dynamic strain amplitude, driving frequency and iron particle content on the damping properties of MREs. Sun *et al* [18] also reported the damping properties of isotropic and structured MREs. The influences of iron particle content, strain amplitude, frequency and magnetic

[3] Authors to whom any correspondence should be addressed.

field were experimentally investigated. These studies have laid the foundation for the investigation of MRE damping properties. However, for the mechanism of MRE damping properties, there are still many key issues that need to be further investigated.

It is known that the damping properties of composites reflect the ability of energy dissipation of materials [19]. In MREs, the energy dissipation mainly comes from the matrix and the interfaces between the matrix and the particles. For the same kind of matrix, the interfaces play an important role in interfacial friction. The interfacial adhesion was enhanced by adding maleic anhydride, which resulted in the reduction of the loss factor [20]. Also, the interfacial area cannot be disregarded. The smaller the interfacial area is, the less the interfacial friction will be.

In this study, two kinds of carbonyl iron particles with different particle sizes were used to obtain different interfacial areas between the matrix and the particles in MREs. Samples with different contents of particles were fabricated. The microstructures of the samples were observed, and the loss factors of the samples were tested and compared. The interfacial friction damping properties of MREs were also investigated.

2. Experimental details

2.1. Preparation of MREs

The matrix material used in this study was cis-polybutadiene rubber (BR), purchased from Shanghai Gao-Qiao Petrochemical Corporation, China. Two different sizes of carbonyl iron particles were used, i.e. 1.1 μm (type HQ-I) and 9 μm (type SL) in diameter, which were bought from BASF. Two groups of MRE samples were fabricated with the HQ-I and SL particles, respectively. Each group consists of four samples with particle weight fractions of 10%, 30%, 60% and 80%, respectively.

The fabrication of MREs consists of mixing, pre-forming configuration and curing. Firstly, 100 phr rubber, 100 phr plasticizer, 14 phr other additives and the iron particles were mixed homogeneously using a two-roll mill (Taihu Rubber Machinery Inc., China, Model XK-160), in which phr is the weight parts based on per hundred parts of rubber. Then, the mixture was put into a mold for pre-forming under an external magnetic field of 1300 mT, generated by our developed magnet–heat couple device [21], at 130 °C for 10 min. Finally, the samples were vulcanized on a flat vulcanizer (Bolon Precision Testing Machines Co., China, Model BL-6170-B). The vulcanization process was operated under a pressure of approximately 13 MPa and at 160 °C for 15 min.

2.2. Observation of microstructure

The microstructures of the samples were observed by using a scanning electron microscope (SEM) machine from FEI Co. (model Sirion200). The accelerating voltage was set at 5 kV. These samples were cut into flakes and coated with a thin layer of gold prior to SEM observation.

2.3. Measurement of dynamic properties

Dynamic mechanical properties of these samples were measured by using a modified dynamic mechanical analyzer (DMA) [21]. In this system, a self-made electromagnet which can generate a variable magnetic field from 0 to 1000 mT was attached to a normal DMA (Triton Technology Ltd, UK, model Tritec 2000B).

In the experiments, the MRE samples had dimensions of 10 mm × 10 mm × 3 mm, in which the particle chains were distributed along the thickness direction. At room temperature, both magnetic field sweep testing (field range 0–1000 mT) and shear strain amplitude sweep testing (strain range 0.1%–2.0%) were employed to measure dynamic properties, such as shear storage modulus and loss factor. The magnetic field and the shear stress were parallel and perpendicular with the direction of the particle chains, respectively. The magnetic field sweep testing was conducted at a frequency of 10 Hz and constant shear strain amplitude of 0.5%. The shear strain amplitude sweep testing was conducted at a frequency of 10 Hz and a magnetic field of 0 mT.

3. Results and discussion

3.1. Microstructure

Figure 1 shows the SEM micrographs of MRE samples, where (a)–(d) samples with 1.1 μm iron particles correspond to the particle weight fractions of 10%, 30%, 60% and 80%, respectively, and (a′)–(d′) samples with 9.0 μm iron particles correspond to the particle weight fractions of 10%, 30%, 60% and 80%, respectively. When the weight fraction of particles is 10%, the particles disperse uniformly and form perfect chains in the matrix, as shown in figures 1(a) and (a′). As the weight fraction of particles increases to 30%, 1.1 μm iron particles agglomerate while 9.0 μm iron particles do not, which can be seen from figures 1(b) and (b′). When the particle weight fraction further increases to 60%, 1.1 μm iron particles agglomerate significantly while 9.0 μm iron particles have almost no agglomeration in the matrix (see figures 1(c) and (c′)). For the MREs with as high as 80% weight fraction of particles, the densely distributed particles are clearly seen in the matrix and the direction of particle chains is illegible (see figures 1(d) and (d′)). Boczkowska *et al* [22] reported that the MREs with high content of iron particles showed a microstructure similar to the three-dimensional lattices of iron particles. The structural and magnetic anisotropy has not been observed. Thus, the complex three-dimensional structures of particles in the matrix might have formed when the particle weight fraction was 80%.

Figure 2 shows the relationship between the shear storage modulus and the weight fractions of particles under zero-field. It can be seen that the zero-field shear storage modulus of the samples with 1.1 μm iron particles is larger than that of the samples with 9.0 μm iron particles. The relative difference of shear storage modulus at the zero-field between two group samples is defined as $R\Delta G_0 = (G_0^{1.1} - G_0^{9.0})/G_0^{9.0}$, in which $G_0^{1.1}$ and $G_0^{9.0}$ are the zero-field shear storage modulus of the samples with 1.1 μm and 9.0 μm iron particles, respectively.

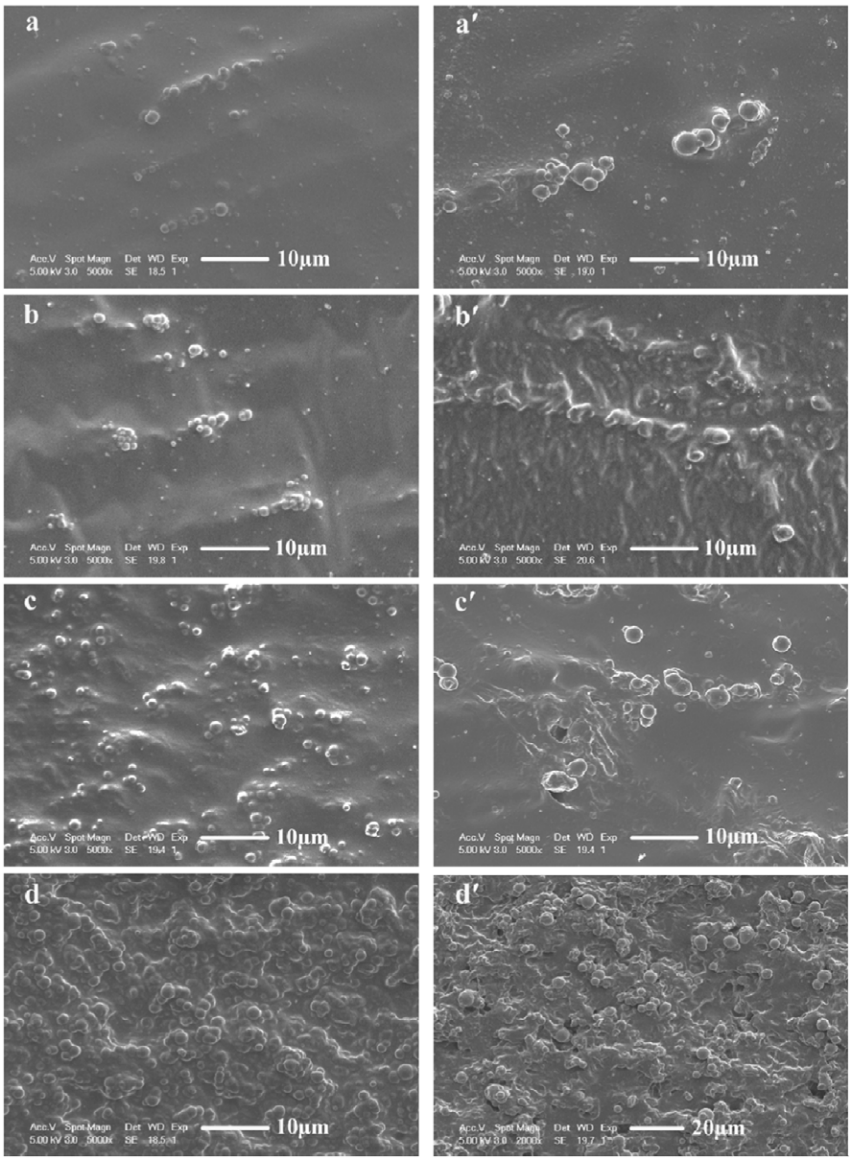

Figure 1. SEM images of the samples with different particle sizes and particle contents: (a)–(d) samples with 1.1 μm iron particles, respectively correspond to the weight fractions of 10%, 30%, 60% and 80% particles; (a′)–(d′) samples with 9.0 μm iron particles, respectively correspond to the weight fractions of 10%, 30%, 60% and 80% particles.

Table 1 shows the relative difference of the shear storage modulus at the zero-field between two group samples under different iron particle contents. When the weight fraction of particles increases from 10% to 80%, $R\Delta G_0$ increases from 0.5% up to 13.3% and then decreases to 3.7%.

Figure 3 shows the sketch of the distribution of iron particles with different particle contents under a magnetic field, where (a)–(d) distributions of 1.1 μm particles correspond to the weight fractions of 10%, 30%, 60% and 80% particles, respectively, and (a′)–(d′) distributions of 9.0 μm particles correspond to the weight fractions of 10%, 30%, 60% and 80% particles, respectively. As can be seen, the particles form chains along the magnetic field direction, in which the 1.1 μm iron particles have obvious agglomeration while the 9.0 μm iron particles disperse uniformly in the matrix as the content of iron particles increases (see figures 3(a)–(d) and (a′)–(d′)). When the iron particles agglomerate in the matrix, some rubber segments will be entrapped among the particles, as shown in figure 3(e). The rubber which is located outside the agglomerate is defined as free rubber, while the rubber which is located inside the agglomerate is defined as restrained rubber.

Table 1. The relative difference of the shear storage modulus at the zero-field between two group samples with different particle contents.

	Relative difference in zero-field shear storage modulus (%)
Weight fraction of carbonyl iron particles (%)	$R\Delta G_0 = (G_0^{1.1} - G_0^{9.0})/G_0^{9.0}$
10	0.5
30	1.9
60	13.3
80	3.7

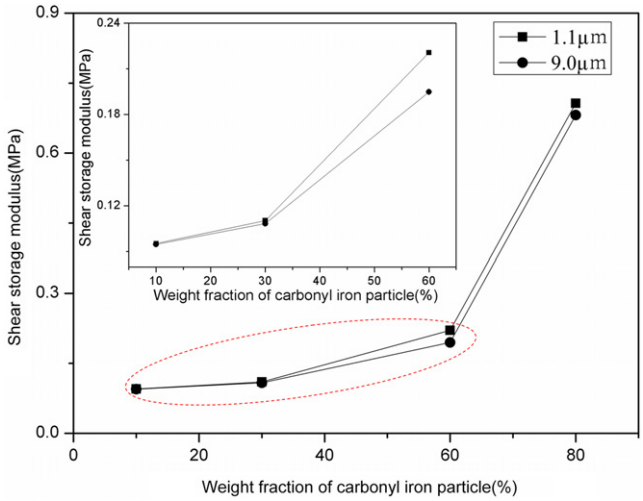

Figure 2. The shear storage modulus of the samples with different particle sizes as a function of particle contents under zero-field.

Under a certain shear stress, the force acts on the restrained rubber usually after overcoming the interactions between the free rubber and the particles as well as between the particles. The movement of the restrained rubber molecule chains is restrained. Thus the storage modulus of restrained rubber is higher than the free rubber. Li *et al* [23] reported that the restrained rubber has made the zero-field shear storage modulus increased in MREs. The more the agglomeration is, the more restrained rubber there will be. Therefore, the $R\Delta G_0$ increases as the contents of iron particles increase from 10% to 60%. However, the distance between the particles in three-dimensional space in the matrix becomes very small when the content of carbonyl iron particles is up to 80% and the restrained rubber can be formed between adjacent particles in the sample with 9.0 μm iron particles (see figure 3(d′) in the red cycle). The zero-field shear storage modulus of the sample with 9.0 μm iron particles can be increased because of the restrained rubber. So the $R\Delta G_0$ has a certain decline at 80% of the particle content.

3.2. Loss factor

Figure 4 shows the loss factors of the samples as a function of magnetic field strength, in which (a)–(d) samples correspond to the weight fractions of 10%, 30%, 60% and 80% particles, respectively. All tests were conducted at a frequency of 10 Hz and constant shear strain amplitude of 0.5%.

The compatibility between inorganic and organic materials is always poor [24, 25]. The MREs will generate the interfacial friction under a shear stress. The energy dissipation of MREs can be expressed as

$$D = D_{\mathrm{m}} + D_{\mathrm{p}} + D_{\mathrm{s}}, \tag{1}$$

where D_{m}, D_{p} and D_{s} are the energy dissipation of the matrix, the particles and the interfacial sliding, respectively. The particle energy dissipation can be ignored compared with the others, so equation (1) can be simplified into

$$D = D_{\mathrm{m}} + D_{\mathrm{s}}. \tag{2}$$

When the particles disperse uniformly and form chains in the matrix, the matrix belongs to the free rubber, that is to say $D_{\mathrm{m}} = D_{\mathrm{fr}}$. Equation (2) can be expressed as

$$D = D_{\mathrm{fr}} + D_{\mathrm{fr-p}} \tag{3}$$

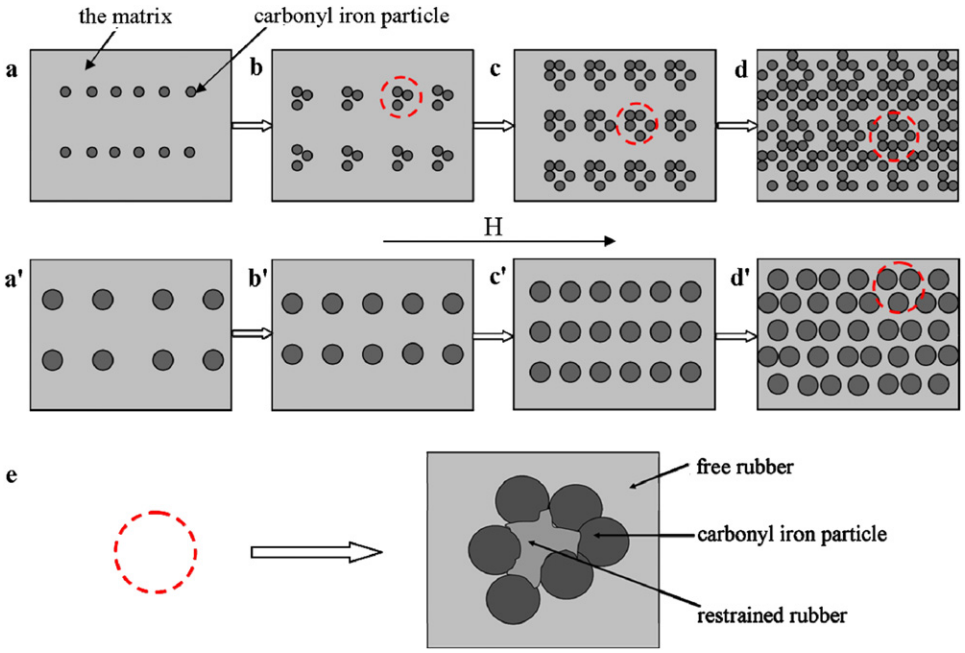

Figure 3. The sketch of the distribution of particles with different particle contents under a magnetic field: (a)–(d) distributions of 1.1 μm particles, respectively correspond to the weight fractions of 10%, 30%, 60% and 80% particles; (a′)–(d′) distributions of 9.0 μm particles, respectively correspond to the weight fractions of 10%, 30%, 60% and 80% particles; (e) the restrained rubber and the free rubber in the red cycle.

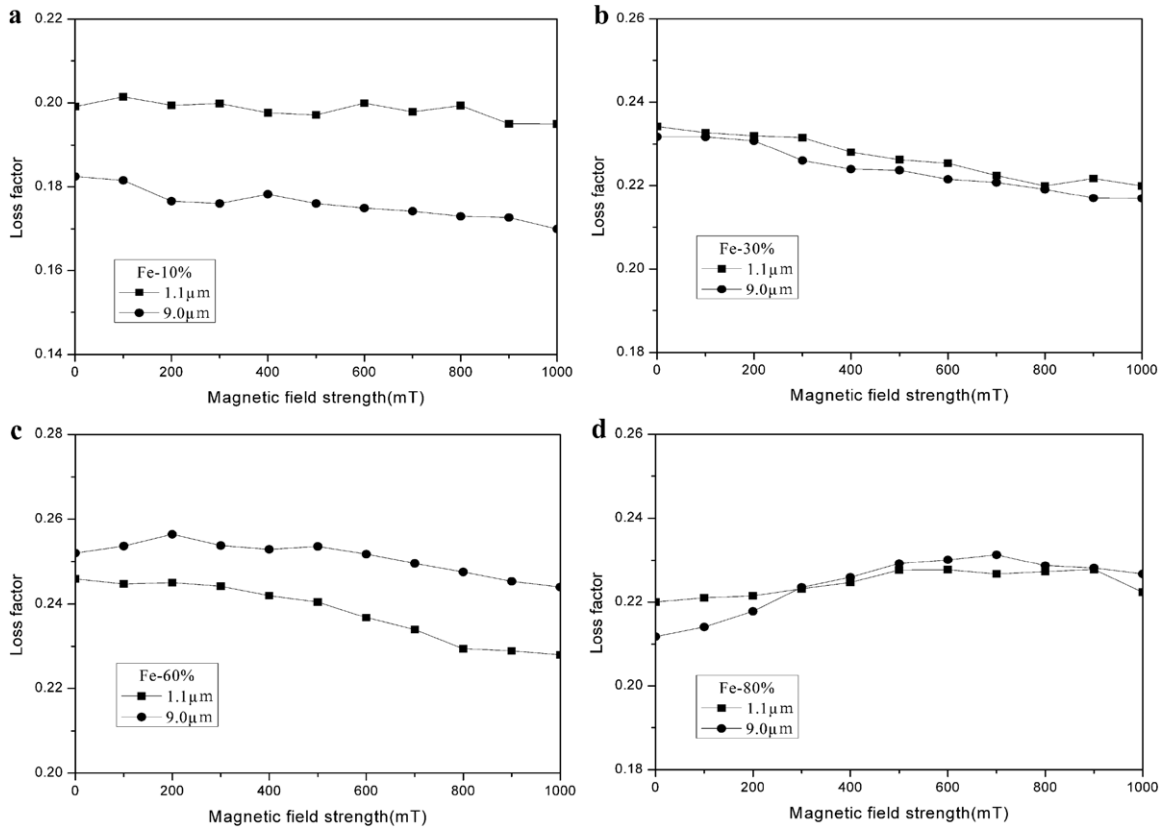

Figure 4. The loss factors of the samples with different particle sizes as a function of magnetic field strength: (a)–(d) samples respectively correspond to the weight fractions of 10%, 30%, 60% and 80% particles.

in which D_{fr} and $D_{\mathrm{fr-p}}$ are the energy dissipation of the free rubber and the interfacial friction between the free rubber and the particles, respectively. When the particles agglomerate in the matrix, the matrix constitutes of the free rubber and the restrained rubber, that is to say $D_{\mathrm{m}} = D_{\mathrm{fr}} + D_{\mathrm{re}}$. The sample owns the interfaces between the free rubber and the particles, between the particles as well as between the restrained rubber and the particles; that is $D_{\mathrm{s}} = D_{\mathrm{fr-p}} + D_{\mathrm{p-p}} + D_{\mathrm{re-p}}$. Equation (2) can be expressed as

$$D = D_{\mathrm{fr}} + D_{\mathrm{re}} + D_{\mathrm{fr-p}} + D_{\mathrm{p-p}} + D_{\mathrm{re-p}}. \tag{4}$$

Here, D_{re} is the energy dissipation of the restrained rubber. $D_{\mathrm{p-p}}$, $D_{\mathrm{re-p}}$ are the energy dissipation of the interfacial friction between the particles as well as between the restrained rubber and the particles, respectively. The movement of the restrained rubber molecule chains is restrained, so the energy dissipation of the restrained rubber can be ignored. Moreover, in the agglomeration, the type of contact between the particles is spot contact, which can be ignored compared with the surface contact between the matrix and the particles. So equation (4) can be simplified into

$$D = D_{\mathrm{fr}} + D_{\mathrm{fr-p}} + D_{\mathrm{re-p}}. \tag{5}$$

Figure 4(a) shows the loss factors of the samples with different particle sizes when the weight fraction of particles is 10%. As can be seen, the loss factor of the sample with 1.1 μm iron particles is higher than that of the sample with 9.0 μm iron particles remarkably. It is known that the smaller the particle size, the larger the surface area. Moreover, two kinds of particles disperse uniformly and form chains in the matrix, and the matrix belongs to the free rubber, as shown in figures 1(a) (a′) and 3(a) (a′). So the sample with 1.1 μm iron particles has larger interfacial area between the free rubber and the particles than the sample with 9.0 μm iron particles. In equation (3), the energy dissipation of the interfacial friction ($D_{\mathrm{fr-p}}$) of the sample with 1.1 μm iron particles will be higher. The matrix of two samples is the same. Therefore, the loss factor of the sample with 1.1 μm iron particles is higher than the one with 9.0 μm.

In figure 4(b), it is noted that the loss factors of two samples are close to each other with 30% weight fraction of particles. The smaller the particle size, the more easily the particles agglomerate. The microstructures of MRE samples are shown in figures 1(b) and (b′), the 1.1 μm iron particles have agglomeration in the matrix. If interfacial sliding occurs at the interfaces between the free rubber and the particles, as well as between the restrained rubber and the particles, the $D_{\mathrm{fr-p}} + D_{\mathrm{re-p}}$ of the sample with 1.1 μm iron particles will be larger than the $D_{\mathrm{fr-p}}$ of the sample with 9.0 μm iron particles, because the sample with 1.1 μm iron particles has a larger interface area, that is to say the loss factor of the sample with 1.1 μm iron particles will be higher. So the interfacial sliding may mainly occur at the interfaces between the free rubber and the particles, that is the $D_{\mathrm{re-p}}$ can be ignored and

equation (5) can be simplified into equation (3). Thus the $D_{\mathrm{fr-p}}$ of the sample with 1.1 μm iron particles will be reduced for the decreased interface area between the free rubber and the particles. The loss factor also can be reduced for the reduced free rubber. In contrast, the sample with 9.0 μm iron particles has no agglomeration, so the loss factor will not be reduced. Therefore, the loss factors of the two samples can be close to each other.

In contrast to figure 4(a), the relationship between the two samples' loss factors shows reverse performance when the content of particles is 60%, in which the loss factor of the sample with 9.0 μm iron particles is higher, as shown in figure 4(c). Figures 1(c) and (c′) and 3(c) and (c′) show that the 1.1 μm iron particles agglomerate significantly, while the 9.0 μm iron particles have almost no agglomeration. For the samples with 9.0 μm iron particles, the loss factor of the sample with 60% iron particles is higher than that of the sample with 30% iron particles for the increased interfacial area between the free rubber and the particles. At the same time, the loss factor of the sample with 60% iron particles (1.1 μm) is also higher than that of the sample with 30% iron particles (1.1 μm). However, when the particle content is 60%, the sample with 1.1 μm iron particles has much restrained rubber, which can reduce the interfacial area between the free rubber and the particles as well as the amount of free rubber. So the increasing range of loss factor of the sample with 1.1 μm iron particles is smaller than that of the sample with 9.0 μm iron particles. The relationship between the two samples' loss factors reaches a critical value when the particle content is 30%. Thus the loss factor of the sample with 1.1 μm iron particles is lower than that of the sample with 9.0 μm iron particles when the particle content is 60%.

With further increasing of the particle content, the distance between the particles becomes smaller in the three-dimensional direction, and the restrained rubber can be formed between the particles. The small distance between particles results in the formation of the restrained rubber in the sample with 9.0 μm iron particles, and the sample with 1.1 μm iron particles has more restrained rubber when the weight fraction of particles is 80%, as shown in figures 1(d) and (d′) and 3(d) and (d′). The restrained rubber can reduce the interfacial area between the free rubber and the particles as well as the amount of free rubber, thus the $D_{\mathrm{fr-p}}$ and the D_{fr} will be decreased. Comparing figures 4(a)–(d), it can be observed that the loss factors of the samples with 80% iron particles are lower than those of the samples with 30% and 60% iron particles. When the content of particles is low, the loss factor increases with the increasing of the particle content. It is indicated that interfacial friction plays an important role in increasing the damping properties of MREs. While the content of particles is up to 80%, the loss factor decreases. This shows that the restrained rubber plays a key role in decreasing damping properties. The loss factors of two samples tend to be consistent nearly under different magnetic field strength, which is closely related to the increased restrained rubber for high particle content, as shown in figure 4(d).

As can be seen in figure 4, under different particle contents, the loss factors of the samples show different tendencies with the increased magnetic field strength. When a magnetic field was applied to the MREs sample, a magnetic interaction force between the particles occurs which can increase the stiffness of MREs, and then obstruct the movement of rubber molecule chains. Thus the energy dissipation of the matrix can be reduced. The interfacial sliding between the free rubber and the particles can be activated totally at or above a critical shear stress. When the shear stress is below the critical value, the interfacial sliding is not activated totally and can continue to slide under an applied magnetic field for the magnetic interaction force between the particles, that is to say the field-induced interfacial sliding. The field-induced interfacial sliding increases with the increased magnetic field until complete activation of the interfaces between the free rubber and the particles. Moreover, the more the particle content, the larger the obstruction effect. The particle content also can affect the critical shear stress. The deformation of the free rubber can reach the shear strain amplitude easily when the particle content is low. While the particle content increases, part of the free rubber deformation cannot reach as much as the shear strain amplitude for the obstruction of particles, then the critical shear stress will increase. Therefore, at certain shear strain amplitude, if interfacial sliding between the free rubber and the particles has been activated, that is the $D_{\mathrm{fr-p}}$ is constant, the obstruction of particles plays a key role in reducing energy dissipation, and the obstruction effect increases with the increased magnetic field until magnetic saturation, that is the D_{fr}, is reduced. So the loss factors show a reduced tendency. If interfacial sliding between the free rubber and the particles has not been activated, the field-induced interfacial sliding plays a key role in increasing energy dissipation first, then the obstruction of particles plays a key role in reducing energy dissipation with the increased magnetic field. Thus the loss factors show a tendency of increase plus decrease. It is noted that if the field-induced interfacial sliding is too small with the increased magnetic field, the obstruction of particles will play a key role and the loss factors show a reduced tendency.

To verify our explanation that interfacial sliding at the interfaces between the free rubber and the particles is dominant for the energy dissipation of interfacial friction, the samples with 30% and 60% particle contents were selected to test their loss factors under different shear strain amplitudes. Figure 5 shows the loss factors of the samples as a function of the shear strain amplitude, in which the increased tendencies of the loss factor with the increased shear strain amplitude can be observed. The tests were conducted at a frequency of 10 Hz and a magnetic field strength of 0 mT. When the shear strain amplitude increases, the movement of the rubber molecule chains and the interfacial sliding between the particles and the matrix will increase, and then the energy dissipation will increase. So the loss factor increases with the increasing of the shear strain amplitude. However, MREs belong to a class of particle reinforced composites, in which the particles in the matrix obstruct the movement of rubber molecule chains. Thus, interfacial sliding between the matrix and the particles plays a main role in energy dissipation. In figure 5(a), the loss factors show the same increased tendencies with the increased

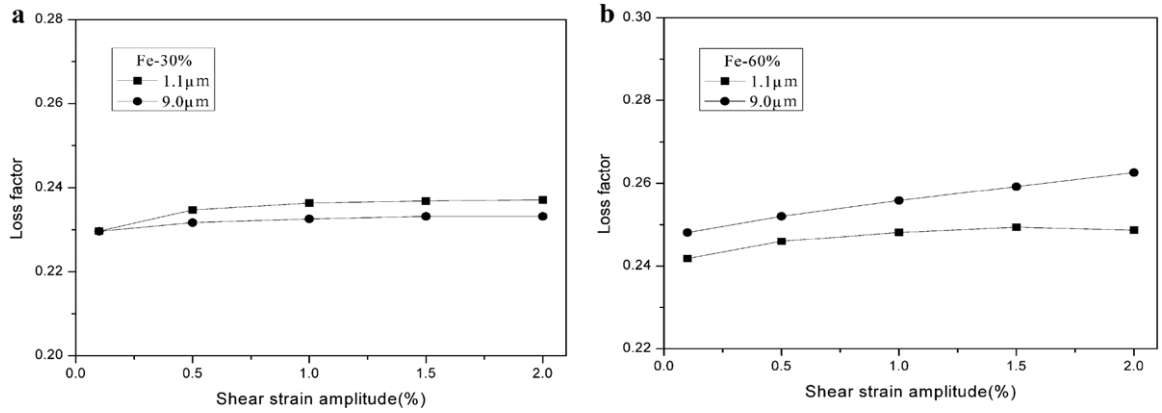

Figure 5. The loss factors of the samples with different particle sizes as a function of the shear strain amplitude: (a) the weight fraction of carbonyl iron particles is 30%; (b) the weight fraction of carbonyl iron particles is 60%.

shear strain amplitude when the particle content is 30%. Above the shear strain amplitude of 0.5%, the loss factors of the two samples tend to be steady, indicating that the interfacial sliding has been activated. The sample with 1.1 μm iron particles has agglomeration while the sample with 9.0 μm iron particles has not (figures 1(b), (b′) and 3(b), (b′)). If interfacial sliding occurs at the interfaces between the free rubber and the particles, as well as between the restrained rubber and the particles with increased shear strain amplitude, the loss factor of the sample with 1.1 μm iron particles will be higher for more interfacial area and tend to be steady at a higher shear strain amplitude because the destruction of the agglomeration needs larger shear stress. Furthermore, figure 5(a) shows that the loss factors of the two samples are close to each other, which is consistent with figure 4(b). This is related to the interfaces between the free rubber and the particles. So interfacial sliding may mainly occur at the interfaces between the free rubber and the particles.

When the content of particles is 60%, it is noted that the increased tendencies of loss factor with the increased shear strain amplitude are different, as shown in figure 5(b). The loss factor of the sample with 9.0 μm iron particles shows a linearly increased tendency while that of the sample with 1.1 μm iron particles shows a gradually stabilized tendency, by which the explanation that interfacial sliding mainly occurs at the interfaces between the free rubber and the particles is further verified. Figures 1(c) and (c′) and 3(c) and (c′) show that the 1.1 μm iron particles agglomerate significantly while the 9.0 μm iron particles do not agglomerate in the matrix. The interfacial area between the free rubber and the particles for the sample with 1.1 μm iron particles will be reduced due to the presence of particle agglomeration. So the loss factor of the sample with 1.1 μm iron particles is lower than that of the sample with 9.0 μm iron particles, which is consistent with figure 4(c). Moreover, the loss factor of the sample with 1.1 μm iron particles shows a plateau above 1.0% shear strain amplitude, while the loss factor of the sample with 9.0 μm iron particles shows a linearly increased tendency. This indicates that the agglomeration in the sample with 1.1 μm iron particles is not destroyed. This further suggests that the interfacial friction damping in our system is mainly from frictional sliding at the interfaces between the free rubber and the particles. In addition, comparing the samples with 60% and 30% particle contents, it is found that the increased tendencies of loss factor with the increased shear strain amplitude are different. As the particle content increases, part of the free rubber deformation cannot reach as much as the shear strain amplitude for the obstruction of particles, and so the critical shear stress will increase. Therefore, compared with the sample with 30% particle content, the interfacial sliding of the sample with 60% particle content is activated at higher shear strain amplitude.

4. Conclusion

In this study, MRE samples with two particle sizes of 1.1 and 9.0 μm as well as different weight fractions of carbonyl iron particles were prepared. The microstructural observations indicate that the 1.1 μm particles have obvious agglomeration in the matrix as the content of particles increases while the 9.0 μm particles do not. The restrained rubber increases gradually with the increased agglomeration. The restrained rubber is formed in the sample with 9.0 μm particles for small distances between particles when the content of particles is 80%. The loss factors were characterized under different magnetic field strength and shear strain amplitudes. The results demonstrate that the relationships between two group samples' loss factors are different as the content of particles increases. The variation of the loss factor depends mainly on the agglomeration of particles in the matrix, because the agglomeration of particles results in the reduced interfacial area between the free rubber and the particles as well as increased restrained rubber. Moreover, the analysis implies that the interfacial friction damping is mainly because of frictional sliding at the interfaces between the free rubber and the particles. These results could be useful in future investigations of MRE damping properties.

Acknowledgments

The financial support from NSFC (grant No. 11072234) and SRFDP of China (project No. 20093402110010) is gratefully acknowledged.

References

[1] Carlson J D and Jolly M R 2000 MR fluid, foam and elastomer devices *Mechatronics* **10** 555–69

[2] Shiga T, Okada A and Kurauchi T 1995 Magnetoviscoelastic behavior of composite gels *J. Appl. Polym. Sci.* **58** 787–92

[3] Farshad M and Le Roux M 2005 Compression properties of magnetostrictive polymer composite gels *Polym. Test.* **24** 163–8

[4] Ginder J M, Nichols M E, Elie L D and Tardiff J L 1999 Magnetorheological elastomers: properties and applications *Proc. SPIE* **3675** 131–8

[5] Li W H, Zhou Y and Tian T F 2010 Viscoelastic properties of MR elastomers under harmonic loading *Rheol. Acta* **49** 733–40

[6] Liu B, Li W H, Kosasih P B and Zhang X Z 2006 Development of an MR-brake-based haptic device *Smart Mater. Struct.* **15** 1960–6

[7] Gong X L, Zhang X Z and Zhang P Q 2005 Fabrication and characterization of isotropic magnetorheological elastomers *Polym. Test.* **24** 669–76

[8] Jolly M R, Carlson J D and Muñoz B C 1996 A model of the behaviour of magnetorheological materials *Smart Mater. Struct.* **5** 607–14

[9] Ginder J M, Schlotter W F and Nichols M E 2001 Magnetorheological elastomers in tunable vibration absorbers *Proc. SPIE* **4331** 103–10

[10] Ginder J M, Clark S M, Schlotter W F and Nichols M E 2002 Magnetostrictive phenomena in magnetorheological elastomers *Int. J. Mod. Phys.* B **16** 2412–18

[11] Deng H X, Gong X L and Wang L H 2006 Development of an adaptive tuned vibration absorber with magnetorheological elastomer *Smart Mater. Struct.* **15** N111–6

[12] Albanese A M and Cunefare K A 2003 Properties of a magnetorheological semiactive vibration absorber *Proc. SPIE* **5052** 36–43

[13] Lerner A A and Cunefare K A 2008 Performance of MRE-based vibration absorbers *J. Intell. Mater. Syst. Struct.* **19** 551–63

[14] Sun H L, Zhang P Q, Gong X L and Chen H B 2007 A novel kind of active resonator absorber and the simulation on its control effort *J. Sound Vib.* **300** 117–25

[15] Hoang N, Zhang N and Du H 2009 A dynamic absorber with a soft magnetorheological elastomer for powertrain vibration suppression *Smart Mater. Struct.* **18** 074009

[16] Demchuk S A and Kuz'min V A 2002 Viscoelastic properties of magnetorheological elastomers in the regime of dynamic deformation *J. Eng. Phys. Thermophys.* **75** 396–400

[17] Chen L, Gong X L and Li W H 2008 Damping of magnetorheological elastomers *Chin. J. Chem. Phys.* **21** 581–5

[18] Sun T L, Gong X L, Jiang W Q, Li J F, Xu Z B and Li W H 2008 Study on the damping properties of magnetorheological elastomers based on cis-polybutadiene rubber *Polym. Test.* **27** 520–6

[19] Chandra R, Singh S P and Gupta K 1999 Damping studies in fiber-reinforced composites—a review *Compos. Struct.* **46** 41–51

[20] Fan Y C, Gong X L, Jiang W Q, Zhang W, Wei B and Li W H 2010 Effect of maleic anhydride on the damping property of magnetorheological elastomers *Smart Mater. Struct.* **19** 055015

[21] Chen L, Gong X L, Jiang W Q, Yao J J, Deng H X and Li W H 2007 Investigation on magnetorheological elastomers based on natural rubber *J. Mater. Sci.* **42** 5483–9

[22] Boczkowska A, Awietjan S F and Wroblewski R 2007 Microstructure-property relationships of urethane magnetorheological elastomers *Smart Mater. Struct.* **16** 1924–30

[23] Li J F, Gong X L, Xu Z B and Jiang W Q 2008 The effect of pre-structure process on magnetorheological elastomer performance *Int. J. Mater. Res.* **99** 1358–64

[24] John M J and Anandjiwala R D 2009 Chemical modification of flax reinforced polypropylene composites *Composites* A **40** 442–8

[25] Sae-oui P, Sirisinha C, Thepsuwan U and Hatthapanit K 2006 Roles of silane coupling agents on properties of silica-filled polychloroprene *Eur. Polym. J.* **42** 479–86